



No random transits in CHEOPS observations of HD 139139^{*,**}




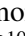

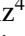
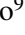

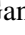


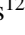





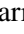
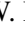
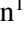
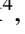
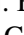

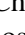




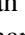


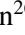

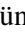


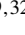
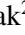






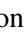
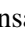
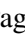



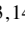









Downloaded from: <https://research.chalmers.se>, 2026-04-05 17:08 UTC

Citation for the original published paper (version of record):

Alonso, R., Hoyer, S., Deleuil, M. et al (2023). No random transits in CHEOPS observations of HD 139139^{*,**}. *Astronomy and Astrophysics*, 680.
<http://dx.doi.org/10.1051/0004-6361/202347779>

N.B. When citing this work, cite the original published paper.

No random transits in CHEOPS observations of HD 139139^{★,★★}

R. Alonso^{1,2}, S. Hoyer³, M. Deleuil³, A. E. Simon⁴, M. Beck⁵, W. Benz^{4,6}, H.-G. Florén⁷,
P. Guterman^{3,8}, L. Borsato⁹, A. Brandeker⁷, D. Gandolfi¹⁰, T. G. Wilson¹¹, T. Zingales^{12,9}, Y. Alibert^{6,4},
G. Anglada^{13,14}, T. Bérczy¹⁵, D. Barrado Navascues¹⁶, S. C. C. Barros^{17,18}, W. Baumjohann¹⁹, T. Beck⁴,
N. Billot⁵, X. Bonfils²⁰, Ch. Broeg^{4,6}, S. Charnoz²¹, A. Collier Cameron¹¹, C. Corral van Damme²²,
Sz. Csizmadia²³, P. E. Cubillos^{24,19}, M. B. Davies²⁵, A. Deline⁵, L. Delrez^{26,27}, O. D. S. Demangeon^{17,18},
B.-O. Demory^{6,4}, D. Ehrenreich^{5,28}, A. Erikson²³, A. Fortier^{4,6}, L. Fossati¹⁹, M. Fridlund^{29,30},
M. Gillon²⁶, M. Güdel³¹, M. N. Günther²², A. Heitzmann⁵, Ch. Helling^{19,32}, K. G. Isaak²²,
L. L. Kiss^{33,34}, E. Kopp³⁵, K. W. F. Lam²³, J. Laskar³⁶, A. Lecavelier des Étangs³⁷, M. Lendl⁵, D. Magrin⁹,
P. F. L. Maxted³⁸, Ch. Mordasini^{4,6}, V. Nascimbeni⁹, G. Olofsson⁷, R. Ottensamer³¹, I. Pagano³⁹,
E. Pallé^{1,2}, G. Peter³⁵, G. Piotto^{9,12}, D. Pollacco⁴⁰, D. Queloz^{41,42}, R. Ragazzoni^{9,12}, N. Rando²²,
H. Rauer^{23,43,44}, I. Ribas^{13,14}, N. C. Santos^{17,18}, G. Scandariato³⁹, D. Ségransan⁵, A. M. S. Smith²³,
S. G. Sousa¹⁷, M. Stalport^{27,26}, Gy. M. Szabó^{45,46}, N. Thomas⁴, S. Udry⁵, B. Ulmer³⁵, V. Van Grootel²⁷,
J. Venturini⁵, F. Verrecchia^{47,48}, and N. A. Walton⁴⁹

(Affiliations can be found after the references)

Received 22 August 2023 / Accepted 12 October 2023

ABSTRACT

Context. The star HD 139139 (a.k.a. ‘the Random Transiter’) is a star that exhibited enigmatic transit-like features with no apparent periodicity in K2 data. The shallow depth of the events (~200 ppm – equivalent to transiting objects with radii of ~1.5 R_{\oplus} in front of a Sun-like star) and their non-periodicity constitute a challenge for the photometric follow-up of this star.

Aims. The goal of this study is to confirm with independent measurements the presence of shallow, non-periodic transit-like features on this object.

Methods. We performed observations with CHEOPS for a total accumulated time of 12.75 days, distributed in visits of roughly 20 h in two observing campaigns in years 2021 and 2022. The precision of the data is sufficient to detect 150 ppm features with durations longer than 1.5 h. We used the duration and times of the events seen in the K2 curve to estimate how many events should have been detected in our campaigns, under the assumption that their behaviour during the CHEOPS observations would be the same as in the K2 data of 2017.

Results. We do not detect events with depths larger than 150 ppm in our data set. If the frequency, depth, and duration of the events were the same as in the K2 campaign, we estimate the probability of having missed all events due to our limited observing window would be 4.8%.

Conclusions. We suggest three different scenarios to explain our results: 1) Our observing window was not long enough, and the events were missed with the estimated 4.8% probability. 2) The events recorded in the K2 observations were time critical, and the mechanism producing them was either not active in the 2021 and 2022 campaigns or created shallower events under our detectability level. 3) The enigmatic events in the K2 data are the result of an unidentified and infrequent instrumental noise in the original data set or its data treatment.

Key words. stars: peculiar – planets and satellites: detection – techniques: photometric

1. Introduction

Thanks to the high precision photometry obtained over hundreds of days with space missions such as *Kepler*/K2 (Borucki et al. 2010; Howell et al. 2014) or TESS (Ricker et al. 2015), a few objects have been observed to exhibit behaviours requiring novel explanations (Boyajian et al. 2016; Rappaport et al. 2019b).

One of the most intriguing cases, HD 139139 (Rappaport et al. 2019a), was observed during K2 Campaign 15 (August 23 to November 20, 2017), displaying a series of 28 transit-like events with shallow depths on the order of 200 ppm and no apparent periodicity during the 87 days of continuous observation. The duration and depth of the transits were different at each event, ranging from 0.7 to 8.2 h and 67 to 408 ppm, respectively. The star shows a 2.7 mag fainter (in G_{RP}) companion at an apparent separation of 3.3'', which is probably physically bound, but it is not clear which star displayed the transit-like events. Among the different scenarios studied in the discovery paper, none was entirely satisfactory. The possible investigated explanations in Rappaport et al. (2019a) included planetary transits in a multiple system, planets orbiting the two stars, a system comprised of

* Raw and de-trended light curves used in this work are available at the CDS via anonymous ftp to cdsarc.cds.unistra.fr (130.79.128.5) or via <https://cdsarc.cds.unistra.fr/viz-bin/cat/J/A+A/680/A78>

** This study uses CHEOPS data obtained as part of the Guaranteed Time Observation (GTO) programme CH_PR110046.

Table 1. Observing log of the CHEOPS visits used in this work.

id #	ObsID	File Key	Start date (UTC)	Obs. efficiency (%)	Visit duration (h)
1	1461054	CH_PR110046_TG000401_V0300	2021-05-01T11:05:38	94.1	19.49
2	1490422	CH_PR110046_TG000501_V0300	2021-05-11T07:50:18	91.3	19.63
3	1489399	CH_PR110046_TG000601_V0300	2021-05-12T14:21:18	91.3	19.63
4	1495676	CH_PR110046_TG000602_V0300	2021-05-17T09:31:17	88.6	19.43
5	1506007	CH_PR110046_TG000701_V0300	2021-06-02T19:06:18	71.9	19.63
6	1502884	CH_PR110046_TG000603_V0300	2021-06-06T22:24:19	72.0	19.63
7	1509091	CH_PR110046_TG000801_V0300	2021-06-08T17:10:18	68.5	22.91
8	1512500	CH_PR110046_TG000901_V0300	2021-06-13T18:33:16	60.6	26.05
9	1783271	CH_PR110046_TG001001_V0300	2022-04-14T02:10:38	71.1	19.43
10	1792614	CH_PR110046_TG001101_V0300	2022-04-27T12:48:40	93.0	19.63
11	1791182	CH_PR110046_TG001201_V0300	2022-04-28T22:19:37	94.1	19.53
12	1797193	CH_PR110046_TG001202_V0300	2022-05-07T12:30:38	91.8	22.18
13	1795741	CH_PR110046_TG001301_V0300	2022-05-09T05:31:39	90.0	19.63
14	1804287	CH_PR110046_TG001501_V0300	2022-05-20T16:53:39	78.1	19.63
15	1808521	CH_PR110046_TG001502_V0300	2022-05-22T10:37:17	80.0	19.63

only a few planets with huge transit timing variations (TTVs), a disintegrating planet, dust-emitting asteroids, S- and P-type planets around binary systems, dipper-like activity, or multiple short-lived star spots. [Schneider \(2019a\)](#) suggested the possibility of one or a few moons with inclined orbits with respect to the orbital plane of a non-transiting planet. This scenario was excluded with a few radial velocity data points that are stable to the 10 m s^{-1} level ([Schneider 2019b](#)), and in that work, three new scenarios were proposed: a belt of eccentric transiter, transits by interstellar objects, or transits by Solar System objects. Due to its enigmatic nature, HD 139139 triggered a radio search for technosignatures using the Green Bank Telescope, resulting in a null detection ([Brzycki et al. 2019](#)).

Another explored possibility in the original paper was that the K2 data suffered from some instrumental effect. Thus, a thorough investigation was performed in order to discard potential instrumental effects, including rolling bands, electronic crosstalk, centroid motion analysis during the dips, and background sources. A sophisticated difference image analysis was consistent with a source of the events located close to the target star, but the saturation and bleeding of the columns in the K2 data complicated the analysis of these images (J. Jenkins, priv. comm.).

The very shallow depths of the transits and their non-periodicity make any ground-based follow-up currently unfeasible. Due to its location near the ecliptic plane, HD 139139 has not been observed with TESS, and it is not scheduled to be observed until at least Sector 86 (October 2024). With the K2 mission now over and the high oversubscription factors of larger space telescopes, there has been no independent confirmation of the intriguing events observed with K2 ('Extraordinary claims require extraordinary evidence', C. Sagan). We describe in this paper our attempt to use the CHaracterising ExOPlanet Satellite (CHEOPS; [Benz et al. 2021](#)) to perform such independent confirmation of the transit-like features on HD 139139.

2. Observations

CHEOPS is the European Space Agency's first S-class mission, and its payload consisted of an optical telescope with an aperture of 30 cm. This telescope is now orbiting on a Sun-synchronous low-Earth orbit at an altitude of 700 km. The design

of the observing strategy was a challenge due to the duration of the events displayed in the K2 curve, lasting between 0.7 and 8.2 h, as well as their intrinsic non-predictability. While a single long visit with a duration of several days is possible using CHEOPS, it would have a non-negligible impact in the other GTO programmes. Moreover, as our aim is to confirm the 'random transiter' behaviour of HD 139139 with an independent instrument, detecting a single event with similar characteristics as those observed in the K2 light curve would suffice for our purpose. If one such event were to be detected at the beginning of a long CHEOPS visit, it would render the observations obtained during the rest of the visit redundant. To avoid this, we adopted the strategy of scheduling one or two weekly visits of 12 continuous orbits each (a duration of about 20 h) at random times when the visibility of the target from CHEOPS was high. The duration of the individual visits would allow for the detection of individual events, and should one be detected, the programme would be stopped, as its main goal would be reached. In case of non-detection of events, we would schedule additional visits (the scheduling at CHEOPS is planned weekly, in nominal conditions) until a total integrated time that allows for a comparison with the K2 light curve was reached. This strategy was followed during two campaigns, one in 2021 and another in 2022. The exposure time was 60 s, as recommended for this $G = 9.56$ star. A summary of the observations and their identifiers are presented in [Table 1](#).

In total, an accumulated time of 6.93 days was acquired in eight visits of roughly 20 h duration in the 2021 campaign, which spanned 44.4 days. The 2022 campaign observed HD 139139 in seven additional visits, accumulating a time of 5.82 days distributed over 39.1 days. The time gap between the 2021 and 2022 campaigns, due to the visibility constraints of CHEOPS, was 303 days.

3. Analysis

The data were processed using the CHEOPS Data Reduction Pipeline (DRP; [Hoyer et al. 2020](#)), version 14.0. In short, the DRP performs an instrumental calibration (bias, gain, linearisation, and flat-fielding correction) and environmental correction (cosmic ray hits, background, and smearing correction) before

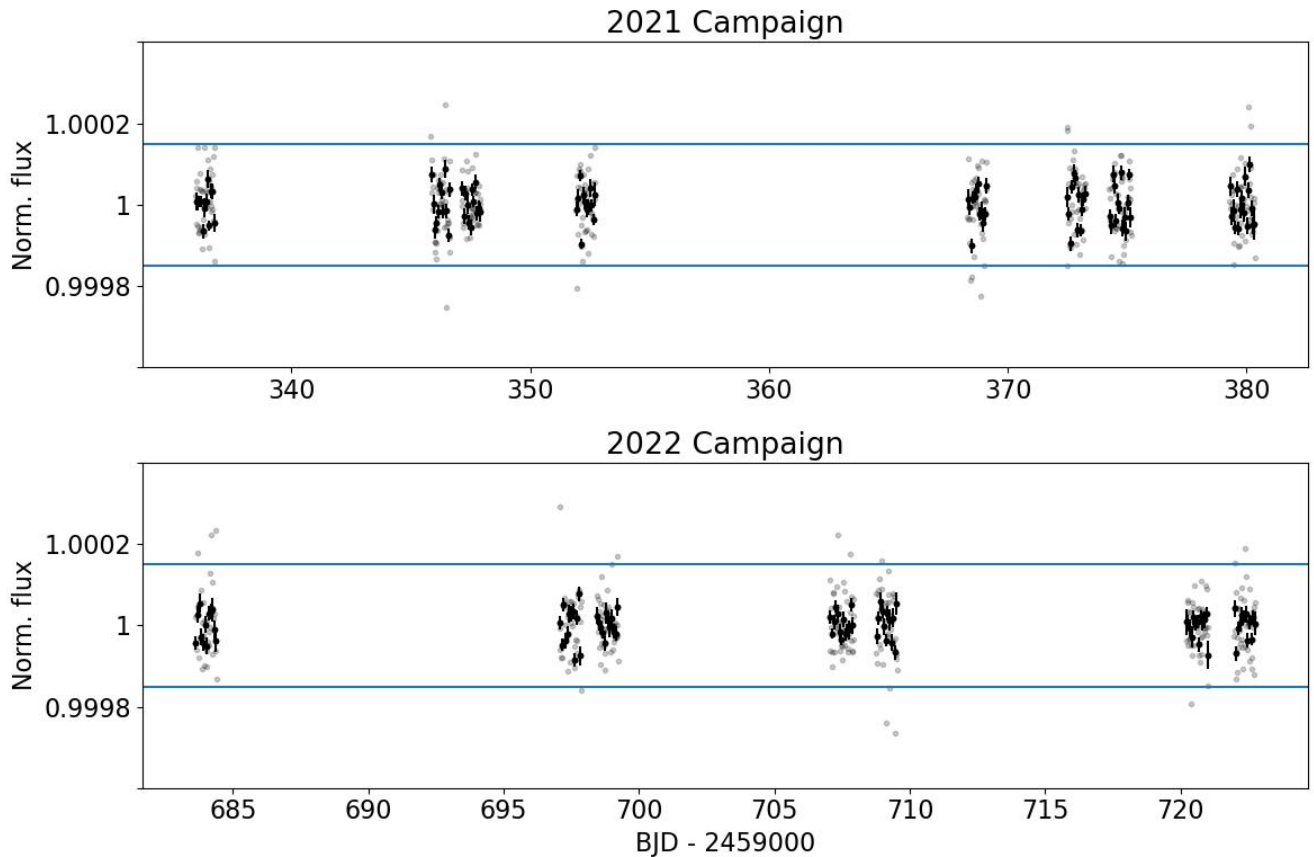


Fig. 1. Light curves of HD 139139 in the two campaigns observed with CHEOPS. The individual exposures have been de-trended against different vectors using `pycheops` (see text for details) and binned to 29 min (grey dots) and one orbit (98.77 min, black dots) for display purposes. The blue horizontal lines represent our detectability limit of 150 ppm, which is smaller than the typical depth of the events detected in K2 data. No points in the one-orbit binned data lie beyond these lines, which we conservatively set as our detectability limit.

extracting the photometric signal of the target in various apertures. After several tests with the different delivered apertures, we selected the R25 (with a radius of 25 px) as the one producing the most precise curves, using the standard deviation of the final curve as a metric. Due to the defocused PSF and the selected radius, the nearby companion of HD 139139 was also included in the photometric aperture. We performed several attempts of using PSF photometry with the PIPE tool¹, but did not obtain better results than the DRP versions. This could be due to the particular configuration of the system, as the nearby contaminant is partially resolved in the images, and it might be confused with PSF distortions by the pipeline. In the regular CHEOPS operations, the location of the sub-window of the CCD that is downlinked is selected as a result of several monitoring and characterisation (M&C) visits designed to track the evolution of the instrument. Several factors are taken into account, including PSF shape, dark current, and the location of hot pixels with respect to the PSF. In a few instances, as a result of these observations, the location of the sub-window was changed². For our observations, the location of the sub-window in each yearly campaign remained constant, but there was a change between the 2021 and 2022 campaigns of 11 px and 2 px in the X and Y coordinates of the detector, respectively. Despite this change, the noise properties of the data obtained in the two campaigns are comparable.

¹ <https://github.com/alphapsa/PIPE>

² <https://www.cosmos.esa.int/web/cheops-guest-observers-programme/in-orbit-updates>

We corrected the DRP data of the remaining systematic effects using the `pycheops` set of tools (Maxted et al. 2022), version 1.1.0. For the sake of homogeneity, we analysed each visit individually using the same de-correlation vectors for all the visits. The raw curves were σ clipped with `clip_outliers` by first using a threshold of 4σ and on a second iteration (after removal of the most obvious outliers and re-determination of the mean absolute deviation) by using a more conservative threshold of 6σ . We masked the data points with background levels above $0.1 e^-$, as these were increasing the final dispersion of the curves. Next, the curves were de-correlated against 13 vectors: linear and quadratic terms in time, X and Y positions in the detector, linear terms in background flux, contamination, smear, $\sin\phi$, $\cos\phi$, $\sin 2\phi$, and $\cos 2\phi$, where ϕ is the satellite's orbital phase. As the typical duration of any event in the K2 light curve was shorter than one CHEOPS visit, which is composed of a minimum of 12 orbits, this correction will have a negligible effect on their detectability. We tested an alternative method to the de-trending described above that models the PSF shape changes using the singular value decomposition of its autocorrelation function, as described in Wilson et al. (2022), but for this particular case, we did not obtain better results than with the `pycheops` de-trended curves, an outcome which is probably also related to the effects of the partially resolved nearby contaminant.

For display purposes, we computed a version in which the data were averaged over one satellite orbit in order to minimise any potential remaining effects at the orbital period. The final light curve is displayed in Fig. 1. The blue horizontal

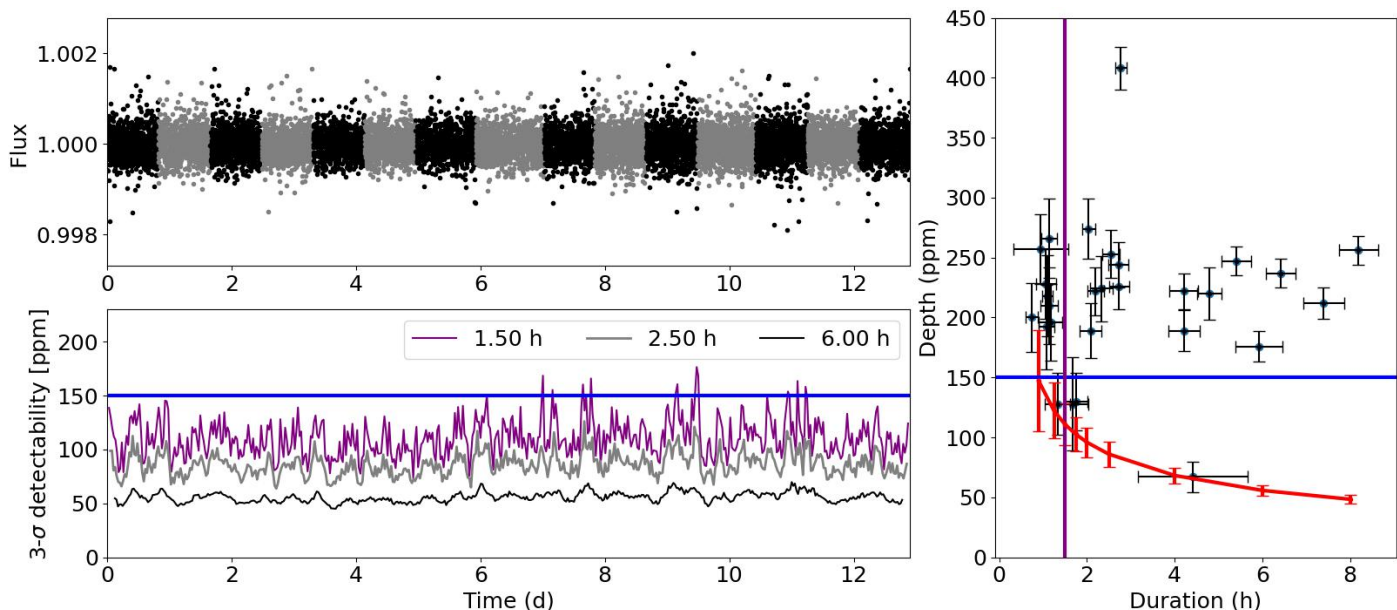


Fig. 2. Establishing the transit-like detectability limits of the CHEOPS observations. The upper-left panel shows the 15 CHEOPS visits stitched together with the original 1 min cadence. From this curve, we estimate the $3\text{-}\sigma$ detectability levels for transits of different durations, as shown in the lower-left panel for a sample of three transit durations. The panel on the right shows the duration and depth of the features reported in the original K2 data (black dots with error bars) and the mean value of the $3\text{-}\sigma$ detectability for different transit durations (red dots and connecting lines). The error bars of the red dots represent the standard deviation of the $3\text{-}\sigma$ detectability curves for each sampled duration. The blue and purple lines represent our selected thresholds for the depth (150 ppm) and duration (1.5 h) of the events that would have been clearly detected in our data. The upper-right quadrant of this panel contains the 16 K2 events that are used to estimate the observation window of our data and to produce the histogram shown in Fig. 3.

lines in the figure encompass a 150 ppm dimming or brightening. There are no one-orbit binned data points beyond these lines in any of the two campaigns, and we conservatively set this as a first threshold for the detection of transit-like events, with a duration of 1.25 CHEOPS orbits or more (~ 2 h), in our data set.

We also constructed versions of the light curves binned to the same cadence as the K2 data (i.e. ~ 29 min). As a measure of the obtained precision, the standard deviation of this light curve is 78 ppm, which is higher than the K2 data by a factor of approximately three. This 29 min cadence light curve is also shown as grey points in Fig. 1. The number of points beyond our threshold of 150 ppm from unity is comparable both below the lower threshold and above the upper threshold, in agreement with the expectations from a constant curve. We also note that there are no consecutive 29 min data points lying beyond our 150 ppm threshold.

Finally, we built a 1 min cadence light curve (i.e. the original cadence), placing the different visits one after the other as if the observations had been performed continuously, with the goal being to better establish the detectability limits. A small gap of 20 min between the visits was included to mimic the effect of the orbital interruptions. The `transit_noise_plot` tool of `pycheops` was used to calculate the noise levels producing 1σ detections of transit features for different durations spanning the interval of 0.9 to 8 h. We used the ‘scaled’ method, in which the transit depth and its standard error are calculated assuming that the true standard errors on the flux measurements are a factor f times the nominal standard error provided by the pipeline. For all the calculated transit durations, this factor was on the order of 1.20 (showing a linear increase from 1.18 for a 0.9 h transit duration to 1.21 for a 8 h duration). The resulting limits at the 3σ level are presented in Fig. 2. Based on these

limits, we set two (conservative) constraints to our detectability levels: 150 ppm in transit depth and 1.5 h in total duration³. With these levels, there are 16 features in the K2 data set that fall safely above the detectability limits. These features were used to estimate the probability of having missed events due to our observing window.

4. Comparison to K2 events

The light curves of both campaigns of CHEOPS data do not show any clear detection of transit-like features similar to those seen in the K2 data. In response to this outcome, we sought to establish whether there is a significant probability of this to happen due not observing long enough or because we were unluckily observing at times when no events were happening. Due to the intrinsic non-predictability of the events and their different individual duration and depths, this was a non-trivial task. Our approach was to replicate a simplified version of the K2 light curve with random starting points for each of the campaigns. The starting points were selected between $t_0 + \Delta t - 87$ and t_0 , where t_0 is the time of the first point in one CHEOPS campaign, Δt is the time span of the observations of one campaign, and 87 days represents the duration of the K2 observations. With these limits, we were assured that a fraction of the K2 light curve was sampled entirely in the Δt of each of the CHEOPS campaigns, which span roughly half the duration of the K2 data.

The central times, duration, and depth of the events contain all the needed information from the K2 light curve for our purpose. For a given starting point, we considered one event as

³ There are a few points in the $3\text{-}\sigma$ detectability curve of the 1.5 h transit duration above the 150 ppm threshold, but these take place mostly at the intersections between visits.

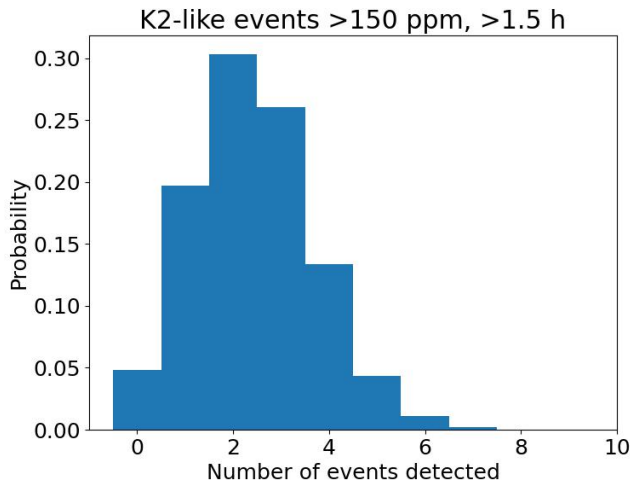


Fig. 3. Histogram of the number of events detected in our observation window, under the assumptions that they share the properties of the ones detected in Rappaport et al. (2019a). From the number of times no events were detected, we estimate the probability of having missed all events in our data set due to our limited observing time to be 4.8%. In this plot, only the K2 features with depths larger than 150 ppm and durations longer than 1.5 h have been considered.

being detected in the CHEOPS data if the number of points (in the 1 min cadence) between the beginning and the end of the event was at least the equivalent to 1.5 h multiplied by the mean observing efficiency of the visits, which is 82.4%. We assumed we were only sensitive to the 16 events in K2 that are both deeper than 150 ppm and longer than 1.5 h, according to the previous results.

We simulated 10 000 curves with random starting points and counted the number of events that were detected with the assumptions above. The result is summarised in the form of a histogram displayed in Fig. 3, and we can estimate the probability to have missed all the events in our observing window as the fraction of times there were no detected events in our simulated curves. Thus, we obtained a probability of 4.8%.

5. Summary and conclusions

We observed HD 139139 for a total accumulated time that should have allowed for the detection of at least one of the most significant events that was seen in the K2 data with a reasonable confidence level (95.2 %). There are a few scenarios that are compatible with these results:

- Our total observing duration still allows for a small probability (which we estimate to be 4.8%) of having missed transit-like features with the same characteristics as those in the K2 data in our window of observations. In the case that these events became less deep or less frequent, as in the epoch of the K2 observations, the probability of having missed them would obviously increase. This was the main driver for performing the 2022 campaign, that is, to increase the confidence in our non-detectability of K2-like events, which has now reached the subjective level inside the GTO team such that no further observations with CHEOPS will be scheduled. We note that the next possibilities are our preferred explanations;
- The events seen in the K2 data were real and ‘active’ at the time of the K2 observations, and they were ‘inactive’ at the

times of CHEOPS observations. There are a few proposed scenarios that could explain this behaviour, such as a cluster of planetesimals or clouds in a shared eccentric orbit that would have transited in 2017 (time of K2 data). Under this scenario, conducting two CHEOPS campaigns in separate years and not finding any transit-like features in the data could be regarded as the potential physical mechanism having a slight preference for periods of non-activity versus activity;

- A subset of the previous scenario would be that while Rappaport et al. (2019a) made a significant effort to discard possible instrumental effects in the K2 data, there is still a possibility that the events in the K2 data set arise from some very infrequent and unidentified noise(s) in that data set. Part of the pixels used in the aperture of the target were exclusively downlinked for the observations of this target (Fig. 6 in Rappaport et al. 2019a), and it was not possible to check for the behaviour of the same pixels in different *Kepler*/K2 pointings. This prevents us from checking if one or a few of these pixels could be malfunctioning (e.g. showing a random telegraphic signal, as in Hoyer et al. 2020). The fact that HD 139139 was saturated and bleeding in the K2 images might have masked such pixels in the core of the stellar image or pixels that were affected by the saturation and bleed.

With our observations not providing an independent confirmation of the enigmatic, random transiter configuration of HD 139139, it is improbable that new CHEOPS campaigns would be dedicated to following the behaviour of the system. Nonetheless, should any other independent data provide further support for the anomalous events seen in the K2 data, we have shown that CHEOPS can reach the precision required for this confirmation.

Acknowledgements. We thank Saul Rappaport, Andrew Vanderburg and Jon Jenkins for a useful discussion on the instrumental analysis performed on the original paper. CHEOPS is an ESA mission in partnership with Switzerland with important contributions to the payload and the ground segment from Austria, Belgium, France, Germany, Hungary, Italy, Portugal, Spain, Sweden, and the United Kingdom. The CHEOPS Consortium would like to gratefully acknowledge the support received by all the agencies, offices, universities, and industries involved. Their flexibility and willingness to explore new approaches were essential to the success of this mission. R.AL, D.Ba., E.Pa., and I.Ri. acknowledge financial support from the Agencia Estatal de Investigación of the Ministerio de Ciencia e Innovación MCIN/AEI/10.13039/501100011033 and the ERDF “A way of making Europe” through projects PID2019-107061GB-C61, PID2019-107061GB-C66, PID2021-125627OB-C31, and PID2021-125627OB-C32, from the Centre of Excellence “Severo Ochoa” award to the Instituto de Astrofísica de Canarias (CEX2019-000920-S), from the Centre of Excellence “María de Maeztu” award to the Institut de Ciències de l’Espai (CEX2020-001058-M), and from the Generalitat de Catalunya/CERCA programme. S.H. gratefully acknowledges CNES funding through the grant 837319. This project was supported by the CNES. L.Bo., T.Zi., V.Na., I.Pa., G.Pi., R.Ra., and G.Sc. acknowledge support from CHEOPS ASI-INAF agreement no. 2019-29-HH.0. A.Br. was supported by the SNSA. D.G. gratefully acknowledges financial support from the CRT foundation under Grant no. 2018.2323 “Gaseous rocky” Unveiling the nature of small worlds”. T.Wi. and A.C.Ca. acknowledge support from STFC consolidated grant numbers ST/R000824/1 and ST/V000861/1, and UKSA grant number ST/R003203/1. Y.Al. acknowledges support from the Swiss National Science Foundation (SNSF) under grant 200020_192038. S.C.C.B. acknowledges support from FCT through FCT contracts nr. IF/01312/2014/CP1215/CT0004. X.B., S.C., D.G., M.F. and J.L. acknowledge their role as ESA-appointed CHEOPS science team members. This work has been carried out within the framework of the NCCR PlanetS supported by the Swiss National Science Foundation under grants 51NF40_182901 and 51NF40_205606. P.E.C. is funded by the Austrian Science Fund (FWF) Erwin Schrodinger Fellowship, program J4595-N. The Belgian participation to CHEOPS has been supported by the Belgian Federal Science Policy Office (BELSPO) in the framework of the PRODEX Program, and by the University of Liège through an ARC grant for

Concerted Research Actions financed by the Wallonia-Brussels Federation. L.D. is an F.R.S.-FNRS Postdoctoral Researcher. This work was supported by FCT – Fundação para a Ciência e a Tecnologia through national funds and by FEDER through COMPETE2020 – Programa Operacional Competitividade e Internacionalização by these grants: UID/FIS/04434/2019, UIDB/04434/2020, UIDP/04434/2020, PTDC/FIS-AST/32113/2017 & POCI-01-0145-FEDER-032113, PTDC/FIS-AST/28953/2017 & POCI-01-0145-FEDER-028953, PTDC/FIS-AST/28987/2017 & POCI-01-0145-FEDER-028987. O.D.S.D. is supported in the form of work contract (DL 57/2016/CP1364/CT0004) funded by national funds through FCT. B.-O.D. acknowledges support from the Swiss State Secretariat for Education, Research and Innovation (SERI) under contract number MB22.00046. This project has received funding from the European Research Council (ERC) under the European Union’s Horizon 2020 research and innovation programme (project FOUR ACES. grant agreement no. 724427). It has also been carried out in the frame of the National Centre for Competence in Research PlanetS supported by the Swiss National Science Foundation (SNSF). DE acknowledges financial support from the Swiss National Science Foundation for project 200021_200726. M.F. and C.M.P. gratefully acknowledge the support of the Swedish National Space Agency (DNR 65/19, 174/18). M.G. is an F.R.S.-FNRS Senior Research Associate. M.N.G. is the ESA CHEOPS Project Scientist and Mission Representative, and as such also responsible for the Guest Observers (GO) Programme. M.N.G. does not relay proprietary information between the GO and Guaranteed Time Observation (GTO) Programmes, and does not decide on the definition and target selection of the GTO Programme. C.He. acknowledges support from the European Union H2020-MSCA-ITN-2019 under Grant Agreement no. 860470 (CHAMELEON). K.G.I. is the ESA CHEOPS Project Scientist and is responsible for the ESA CHEOPS Guest Observers Programme. She does not participate in, or contribute to, the definition of the Guaranteed Time Programme of the CHEOPS mission through which observations described in this paper have been taken, nor to any aspect of target selection for the programme. K.W.F.L. was supported by Deutsche Forschungsgemeinschaft grants RA714/14-1 within the DFG Schwerpunkt SPP 1992, Exploring the Diversity of Extrasolar Planets. This work was granted access to the HPC resources of MesoPSL financed by the Région Île-de-France and the project Equip@Meso (reference ANR-10-EQPX-29-01) of the programme Investissements d’Avenir supervised by the Agence Nationale pour la Recherche. M.L. acknowledges support of the Swiss National Science Foundation under grant number PCEFP2_194576. P.M. acknowledges support from STFC research grant number ST/M001040/1. This work was also partially supported by a grant from the Simons Foundation (PI Queloz, grant number 327127). N.C.Sa. acknowledges funding by the European Union (ERC, FIERCE, 101052347). Views and opinions expressed are however those of the author(s) only and do not necessarily reflect those of the European Union or the European Research Council. Neither the European Union nor the granting authority can be held responsible for them. S.G.S. acknowledges support from FCT through FCT contract nr. CEECIND/00826/2018 and POPH/FSE (EC). Gy.M.Sz. acknowledges the support of the Hungarian National Research, Development and Innovation Office (NKFIH) grant K-125015, a PRODEX Experiment Agreement No. 4000137122, the Lendület LP2018-7/2021 grant of the Hungarian Academy of Science and the support of the city of Szombathely. V.V.G. is an F.R.S.-FNRS Research Associate. N.A.W acknowledges UKSA grant ST/R004838/1.

References

- Benz, W., Broeg, C., Fortier, A., et al. 2021, *Exp. Astron.*, **51**, 109
- Borucki, W. J., Koch, D., Basri, G., et al. 2010, *Science*, **327**, 977
- Boyajian, T. S., LaCourse, D. M., Rappaport, S. A., et al. 2016, *MNRAS*, **457**, 3988
- Brzycki, B., Siemion, A., Croft, S., et al. 2019, *RNAAS*, **3**, 147
- Howell, S. B., Sobek, C., Haas, M., et al. 2014, *PASP*, **126**, 398
- Hoyer, S., Guterman, P., Demangeon, O., et al. 2020, *A&A*, **635**, A24
- Maxed, P. F. L., Ehrenreich, D., Wilson, T. G., et al. 2022, *MNRAS*, **514**, 77
- Rappaport, S., Vanderburg, A., Kristiansen, M. H., et al. 2019a, *MNRAS*, **488**, 2455
- Rappaport, S., Zhou, G., Vanderburg, A., et al. 2019b, *MNRAS*, **485**, 2681
- Ricker, G. R., Winn, J. N., Vanderspek, R., et al. 2015, *J. Astron. Telesc. Instrum. Syst.*, **1**, 014003
- Schneider, J. 2019a, *RNAAS*, **3**, 108
- Schneider, J. 2019b, *RNAAS*, **3**, 141
- Wilson, T. G., Goffo, E., Alibert, Y., et al. 2022, *MNRAS*, **511**, 1043
- ² Departamento de Astrofísica, Universidad de La Laguna, Astrofísico Francisco Sanchez s/n, 38206 La Laguna, Tenerife, Spain
- ³ Aix-Marseille Univ., CNRS, CNES, LAM, 38 rue Frédéric Joliot-Curie, 13388 Marseille, France
- ⁴ Physikalisches Institut, University of Bern, Gesellschaftsstrasse 6, 3012 Bern, Switzerland
- ⁵ Observatoire Astronomique de l’Université de Genève, Chemin Pegasi 51, 1290 Versoix, Switzerland
- ⁶ Center for Space and Habitability, University of Bern, Gesellschaftsstrasse 6, 3012 Bern, Switzerland
- ⁷ Department of Astronomy, Stockholm University, AlbaNova University Center, 10691 Stockholm, Sweden
- ⁸ Division Technique INSU, CS20330, 83507 La Seyne-sur-Mer cedex, France
- ⁹ INAF, Osservatorio Astronomico di Padova, Vicolo dell’Osservatorio 5, 35122 Padova, Italy
- ¹⁰ Dipartimento di Fisica, Università degli Studi di Torino, Via Pietro Giuria 1, 10125, Torino, Italy
- ¹¹ Centre for Exoplanet Science, SUPA School of Physics and Astronomy, University of St Andrews, North Haugh, St Andrews KY16 9SS, UK
- ¹² Dipartimento di Fisica e Astronomia “Galileo Galilei”, Università degli Studi di Padova, Vicolo dell’Osservatorio 3, 35122 Padova, Italy
- ¹³ Institut de Ciències de l’Espai (ICE, CSIC), Campus UAB, Can Magrans s/n, 08193 Bellaterra, Spain
- ¹⁴ Institut d’Estudis Espacials de Catalunya (IEEC), Gran Capità 2–4, 08034 Barcelona, Spain
- ¹⁵ Admatis, 5. Kandó Kálmán Street, 3534 Miskolc, Hungary
- ¹⁶ Depto. de Astrofísica, Centro de Astrobiología (CSIC-INTA), ESAC campus, 28692 Villanueva de la Cañada (Madrid), Spain
- ¹⁷ Instituto de Astrofísica e Ciências do Espaço, Universidade do Porto, CAUP, Rua das Estrelas, 4150-762 Porto, Portugal
- ¹⁸ Departamento de Física e Astronomia, Faculdade de Ciências, Universidade do Porto, Rua do Campo Alegre, 4169-007 Porto, Portugal
- ¹⁹ Space Research Institute, Austrian Academy of Sciences, Schmiedlstrasse 6, 8042 Graz, Austria
- ²⁰ Université Grenoble Alpes, CNRS, IPAG, 38000 Grenoble, France
- ²¹ Université de Paris Cité, Institut de physique du globe de Paris, CNRS, 1 rue Jussieu, 75005 Paris, France
- ²² European Space Agency (ESA), European Space Research and Technology Centre (ESTEC), Keplerlaan 1, 2201 AZ Noordwijk, The Netherlands
- ²³ Institute of Planetary Research, German Aerospace Center (DLR), Rutherfordstrasse 2, 12489 Berlin, Germany
- ²⁴ INAF, Osservatorio Astrofisico di Torino, Via Osservatorio 20, 10025 Pino Torinese, Italy
- ²⁵ Centre for Mathematical Sciences, Lund University, Box 118, 221 00 Lund, Sweden
- ²⁶ Astrobiology Research Unit, Université de Liège, Allée du 6 Août 19C, 4000 Liège, Belgium
- ²⁷ Space sciences, Technologies and Astrophysics Research (STAR) Institute, Université de Liège, Allée du 6 Août 19C, 4000 Liège, Belgium
- ²⁸ Centre Vie dans l’Univers, Faculté des sciences, Université de Genève, Quai Ernest-Ansermet 30, 1211 Geneva 4, Switzerland
- ²⁹ Leiden Observatory, University of Leiden, PO Box 9513, 2300 RA Leiden, The Netherlands
- ³⁰ Department of Space, Earth and Environment, Chalmers University of Technology, Onsala Space Observatory, 439 92 Onsala, Sweden
- ³¹ Department of Astrophysics, University of Vienna, Türkenschanzstrasse 17, 1180 Vienna, Austria
- ³² Institute for Theoretical Physics and Computational Physics, Graz University of Technology, Petersgasse 16, 8010 Graz, Austria
- ³³ Konkoly Observatory, Research Centre for Astronomy and Earth Sciences, Konkoly Thege Miklós út 15–17, 1121 Budapest, Hungary
- ³⁴ ELTE Eötvös Loránd University, Institute of Physics, Pázmány Péter sétány 1/A, 1117 Budapest, Hungary

¹ Instituto de Astrofísica de Canarias, Vía Láctea s/n, 38200 La Laguna, Tenerife, Spain
e-mail: ras@iac.es

- ³⁵ German Aerospace Center (DLR), Institute of Optical Sensor Systems, Rutherfordstraße 2, 12489 Berlin, Germany
- ³⁶ IMCCE, UMR8028 CNRS, Observatoire de Paris, PSL Univ., Sorbonne Univ., 77 av. Denfert-Rochereau, 75014 Paris, France
- ³⁷ Institut d'astrophysique de Paris, UMR7095 CNRS, Université Pierre & Marie Curie, 98bis blvd. Arago, 75014 Paris, France
- ³⁸ Astrophysics Group, Lennard Jones Building, Keele University, Staffordshire, ST5 5BG, UK
- ³⁹ INAF, Osservatorio Astrofisico di Catania, Via S. Sofia 78, 95123 Catania, Italy
- ⁴⁰ Department of Physics, University of Warwick, Gibbet Hill Road, Coventry CV4 7AL, UK
- ⁴¹ ETH Zurich, Department of Physics, Wolfgang-Pauli-Strasse 2, 8093 Zurich, Switzerland
- ⁴² Cavendish Laboratory, JJ Thomson Avenue, Cambridge CB3 0HE, UK
- ⁴³ Zentrum für Astronomie und Astrophysik, Technische Universität Berlin, Hardenbergstr. 36, 10623 Berlin, Germany
- ⁴⁴ Institut fuer Geologische Wissenschaften, Freie Universitaet Berlin, Maltheserstrasse 74-100, 12249 Berlin, Germany
- ⁴⁵ ELTE Eötvös Loránd University, Gothard Astrophysical Observatory, Szent Imre h. u. 112, 9700 Szombathely, Hungary
- ⁴⁶ HUN-REN-ELTE Exoplanet Research Group, Szent Imre h. u. 112, 9700 Szombathely, Hungary
- ⁴⁷ Space Science Data Center, ASI, via del Politecnico snc, 00133 Roma, Italy
- ⁴⁸ INAF, Osservatorio Astronomico di Roma, Via Frascati 33, 00078 Monte Porzio Catone (RM), Italy
- ⁴⁹ Institute of Astronomy, University of Cambridge, Madingley Road, Cambridge CB3 0HA, UK